Available online at www.sciencedirect.com

ScienceDirect

www.elsevier.com/locate/brainres

Research Report

Neural mechanisms of phonemic restoration for speech comprehension revealed by magnetoencephalography ☆

Kishiko Sunami[a,*], Akira Ishii[b], Sakurako Takano[a], Hidefumi Yamamoto[a], Tetsushi Sakashita[a], Masaaki Tanaka[b], Yasuyoshi Watanabe[b,c], Hideo Yamane[a]

[a]Department of Otorhinolaryngology, Osaka City University Graduate School of Medicine, 1-4-3 Asahimachi, Abeno-ku, Osaka 545-8585, Japan

[b]Department of Physiology, Osaka City University Graduate School of Medicine, 1-4-3 Asahimachi, Abeno-ku, Osaka 545-8585, Japan

[c]RIKEN Center for Life Science Technologies, 6-7-3 Minatojima-minamimachi, Chuo-ku, Hyogo 650-0047, Japan

ARTICLE INFO

Article history:
Accepted 11 September 2013
Available online 18 September 2013

Keywords:
Hearing loss
Magnetoencephalography (MEG)
Phonemic restoration
Speech comprehension

ABSTRACT

In daily communication, we can usually still hear the spoken words as if they had not been masked and can comprehend the speech when spoken words are masked by background noise. This phenomenon is known as phonemic restoration. Since little is known about the neural mechanisms underlying phonemic restoration for speech comprehension, we aimed to identify the neural mechanisms using magnetoencephalography (MEG). Twelve healthy male volunteers with normal hearing participated in the study. Participants were requested to carefully listen to and understand recorded spoken Japanese stories, which were either played forward (forward condition) or in reverse (reverse condition), with their eyes closed. Several syllables of spoken words were replaced by 300-ms white-noise stimuli with an inter-stimulus interval of 1.6–20.3 s. We compared MEG responses to white-noise stimuli during the forward condition with those during the reverse condition using time–frequency analyses. Increased 3–5 Hz band power in the forward condition compared with the reverse condition was continuously observed in the left inferior frontal gyrus [Brodmann's areas (BAs) 45, 46, and 47] and decreased 18–22 Hz band powers caused by white-noise stimuli were seen in the left transverse temporal gyrus (BA 42) and superior temporal gyrus (BA 22). These results suggest that the left inferior frontal gyrus and left transverse and superior temporal gyri are involved in phonemic restoration for speech comprehension. Our findings may help clarify the neural mechanisms of phonemic restoration as well as develop innovative treatment methods for individuals suffering from impaired speech comprehension, particularly in noisy environments.

*Corresponding author. Fax: +81 6 6646 0515.
E-mail address: kishiko@med.osaka-cu.ac.jp (K. Sunami).

0006-8993/$ - see front matter © 2013 The Authors. Published by Elsevier B.V. All rights reserved.
http://dx.doi.org/10.1016/j.brainres.2013.09.010

1. Introduction

In our daily communication, spoken words are sometimes masked by background noise. However, even when the spoken words are masked in this way, we can usually still hear the spoken words and comprehend the content of speech as if it were not masked. The auditory system has the capability to restore the interrupted parts of the spoken words, and can help to perceptually restore the masked portions of the spoken words to meaningful speech, using cues such as expectations, linguistic knowledge, syntactic, semantic, and lexical constraints, and context in noisy environments; this phenomenon is known as phonemic restoration (Warren, 1970; Warren et al., 1972, 1997; Warren and Bashford, 1981; Verschuure and Brocaar, 1983; Sivonen et al., 2006; Davis and Johnsrude, 2007).

Some degree of age-related impairment of speech comprehension, particularly in noisy environments, is common among older adults. In this population, in addition to a simple loss of acuity due to loss of cochlear hair cells, higher-level auditory processing deficits may make spoken words unclear or garbled even when properly amplified or corrected by hearing aids (Jerger et al., 1989). Disability of phonemic restoration, which is considered to be caused by hearing loss (Başkent, 2010 and Başkent et al., 2010), could be as one of the primary reasons for impaired speech comprehension in noisy environments (Plomp and Mimpen, 1979, Duquesnoy, 1983, Dubno et al., 1984 and Schneider et al., 2000). Clarifying the neural mechanisms of phonemic restoration thus seems useful to develop treatment methods for those who suffer from impaired speech comprehension, particularly in noisy environments.

Although functional magnetic resonance imaging (fMRI) studies (Petkov et al., 2007a; Riecke et al., 2007; Shahin et al., 2009) have been performed to clarify the neural mechanisms of phonemic restoration, those studies focused solely on the perceived continuity against interrupted noise stimuli. The roles of speech comprehension on phonemic restoration should not be underestimated, and to further clarify the neural mechanisms underlying phonemic restoration, studies focusing on speech comprehension against interrupted noise stimuli would be useful. Neural mechanisms related to the restoration of speech comprehension should thus be clarified. We focused on the neural mechanisms related to the restoration of speech comprehension in healthy young participants in our present study. In addition to the neural activities caused by listening to the noise which interrupts speeches (continual phonemic restoration), we also evaluated the neural activities that were observed throughout listening to the speeches (continuous phonemic restoration), because the neural mechanisms of the phonemic restoration may be related to such as expectations, linguistic knowledge, syntactic, semantic, and lexical constraints, and the neural substrates related to the comprehension of context may be activated not only during the noise stimuli but also during the intervals of the noise stimuli.

In addition to offering high temporal resolution, magnetoencephalography (MEG) has the advantage of measuring brain activity using time–frequency analyses (Stam, 2010). Oscillatory brain rhythms are considered to originate from synchronous synaptic activities of a large number of neurons (Brookes et al., 2011). Synchronization of neural networks may reflect integration of information processing. Such synchronization processes can be evaluated using MEG time–frequency analyses, and multiple, broadly distributed and continuously interacting dynamic neural networks can be identified through the synchronization of oscillations at particular time–frequency bands (Varela et al., 2001). Alterations of MEG power densities in some brain regions and time–frequency bands induced by interrupted noise stimuli when listening to and understanding spoken stories may provide valuable clues to identifying the neural mechanisms of phonemic restoration for speech comprehension. The aim of this study was therefore to clarify the neural mechanisms of phonemic restoration for speech comprehension in healthy young participants, using MEG time–frequency and behavioral analyses in subjects with normal hearing.

2. Results

Pure-tone hearing ability, assessed by the mean of pure-tone thresholds of the right and left ears at 125 Hz, 250 Hz, 500 Hz, 1000 Hz, 2000 Hz, 4000 Hz and 8000 Hz were 6.5 ± 2.9 dB and 5.7 ± 3.4 dB, respectively. Articulation score in speech audiometry of the right and left ears were $97.7 \pm 2.2\%$ and $97.5 \pm 1.9\%$, respectively.

The numbers of correct answer to the questions asked immediately after the end of Story A and Story B, i.e., the objective story-comprehension levels, were 7.1 ± 1.0 and 7.8 ± 0.6, respectively. Subjective story-comprehension levels as assessed by the 5-point scale immediately after the end of Story A and Story B were 3.5 ± 1.0 and 4.3 ± 0.6, respectively.

To identify the time–frequency bands associated with phonemic restoration for speech comprehension, sensor-level time–frequency maps were observed (Fig. 1). In the time–frequency maps, increased 3–5 Hz band powers at 0–400 ms after the onset of white noise relative to baseline (−500 to 0 ms) (Fig. 1A) and decreased 18–22 Hz band powers at 250–500 ms after onset of white noise relative to baseline (−500 to 0 ms) (Fig. 1B) were specifically shown in the forward condition across most participants.

Based on the observation of sensor-level time–frequency maps, we focused on MEG time–frequency analyses with temporal frequency ranges of 3–5 Hz (increased band power) and 18–22 Hz (decreased band power). Statistical parametric maps of band power changes with the time window of 0–1000 ms (every 200 ms) after the onset of white noise relative to baseline (−200 to 0 ms) in the forward condition are shown in Fig. 2, while those in the reverse condition are shown in Fig. 3. Activated various brain regions overlapped between these two conditions.

To identify brain regions associated with the phonemic restoration of speech comprehension (continual phonemic restoration), time–frequency band power changes with the time window of 0–1000 ms (every 200 ms) after the onset of white noise relative to baseline (−200 to 0 ms) in the forward condition compared with the reverse condition were analyzed (Fig. 4 and Table 1; paired *t*-test). Decreased 18–22 Hz

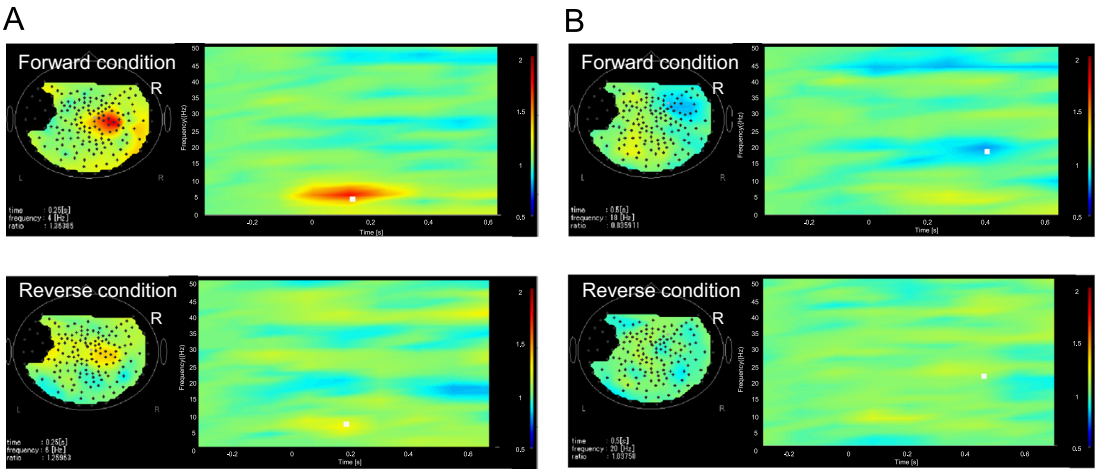

Fig. 1 – Examples of time–frequency representation plot and topography (Subject 6). Changes of 3–5 Hz band powers (A) and 18–22 Hz band powers (B) after the onset of white noise relative to baseline (−500 to 0 ms) in the forward and reverse conditions are shown. The right (R) sides are indicated.

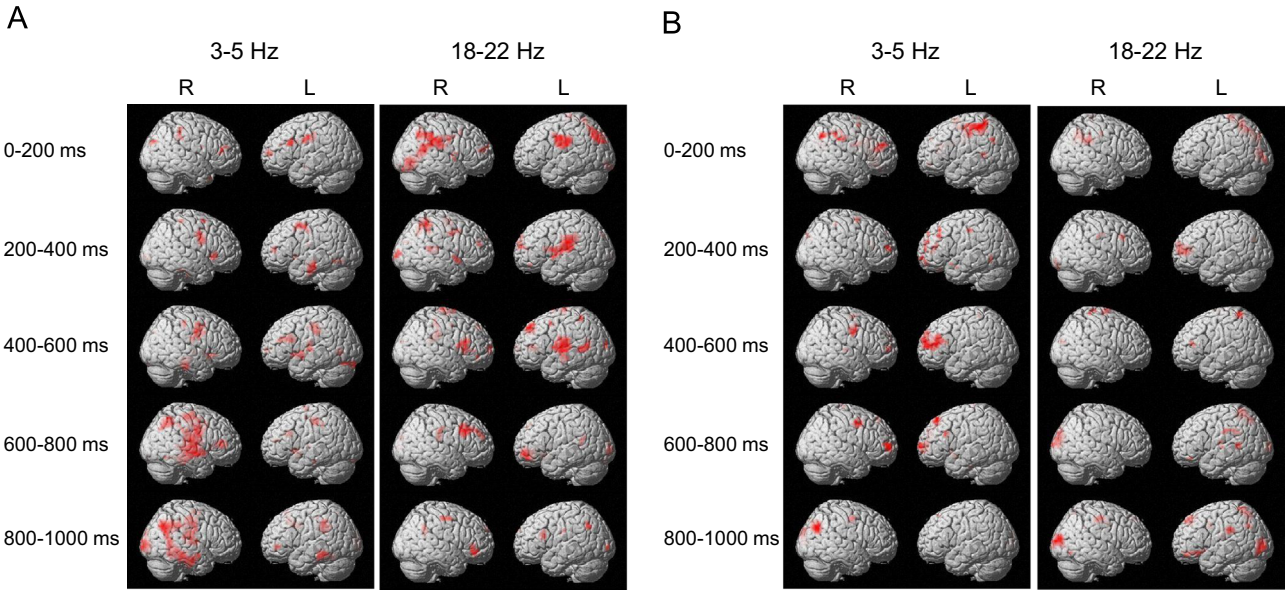

Fig. 2 – Statistical parametric maps of decreased (A) and increased (B) 3–5 Hz and 18–22 Hz band powers after the onset of white noise relative to baseline (−200 to 0 ms) in the forward condition. Statistical parametric maps are superimposed on surface-rendered high-resolution MRI. Brain regions showing decreased (A) or increased (B) band powers are colored in red. The right (R) and left (L) sides are indicated. Random-effect analyses of 12 participants, $P<0.05$, corrected for entire search volumes (family-wise error rate).

band powers were observed in the left transverse temporal gyrus [Brodmann's area (BA) 42] (200–400 and 400–600 ms) and left superior temporal gyrus (BA 22) (200–400 ms). However, increased 3–5 Hz band powers were not identified in any of the brain regions.

Since phonemic restoration for speech comprehension seems to be, at least in part, continuously conducted throughout the forward sessions, i.e., Story A and Story B sessions, the common brain regions activated during the pre- and post-trigger periods are also related to phonemic restoration (continuous phonemic restoration). We therefore analyzed the time–frequency band power changes in the forward condition compared with the reverse condition in the pre-trigger (−500 to 0 ms), post-trigger (0–1000 ms), and total (−500 to 1000 ms) periods, to identify additional brain regions associated with phonemic restoration for speech comprehension (Fig. 5 and Table 2; one-sample *t*-test). Increased 3–5 Hz band powers were observed in the left inferior frontal gyrus (BA 45) and right middle temporal gyrus (BA 39) during the pre-trigger period, in the left inferior frontal gyrus (BA 47) and right inferior temporal gyrus (BA 37) during the post-trigger period, and in the left frontal gyrus (BA 47), right superior frontal gyrus (BA 11), and right middle occipital gyrus (BA 37) during the total period. Decreased 18–22 Hz band powers were shown in the left insula (BA 13) during the pre-trigger period, in the left middle temporal gyrus (BA 21) during the

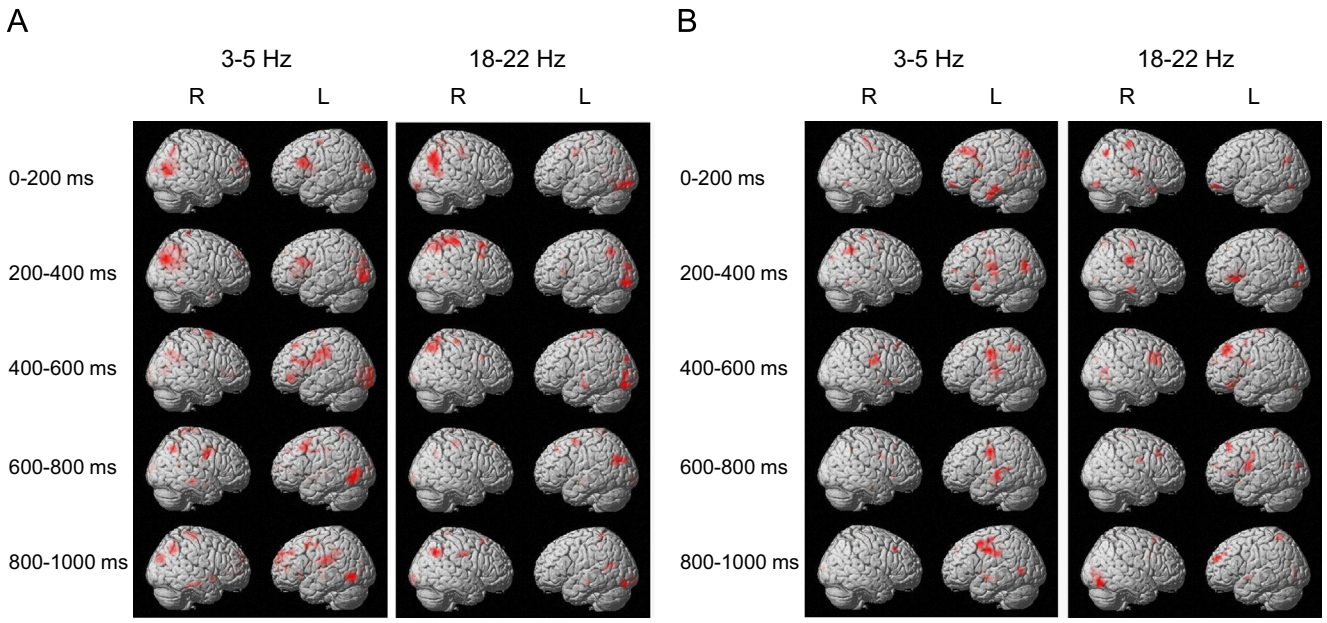

Fig. 3 – Statistical parametric maps of decreased (A) and increased (B) 3–5 Hz and 18–22 Hz band powers after the onset of white noise relative to baseline (−200 to 0 ms) in the reverse condition. Statistical parametric maps are superimposed on surface-rendered high-resolution MRI. Brain regions showing decreased (A) or increased (B) band powers are colored in red. The right (R) and left (L) sides are indicated. Random-effect analyses of 12 participants, $P<0.05$, corrected for the entire search volumes (family-wise error rate).

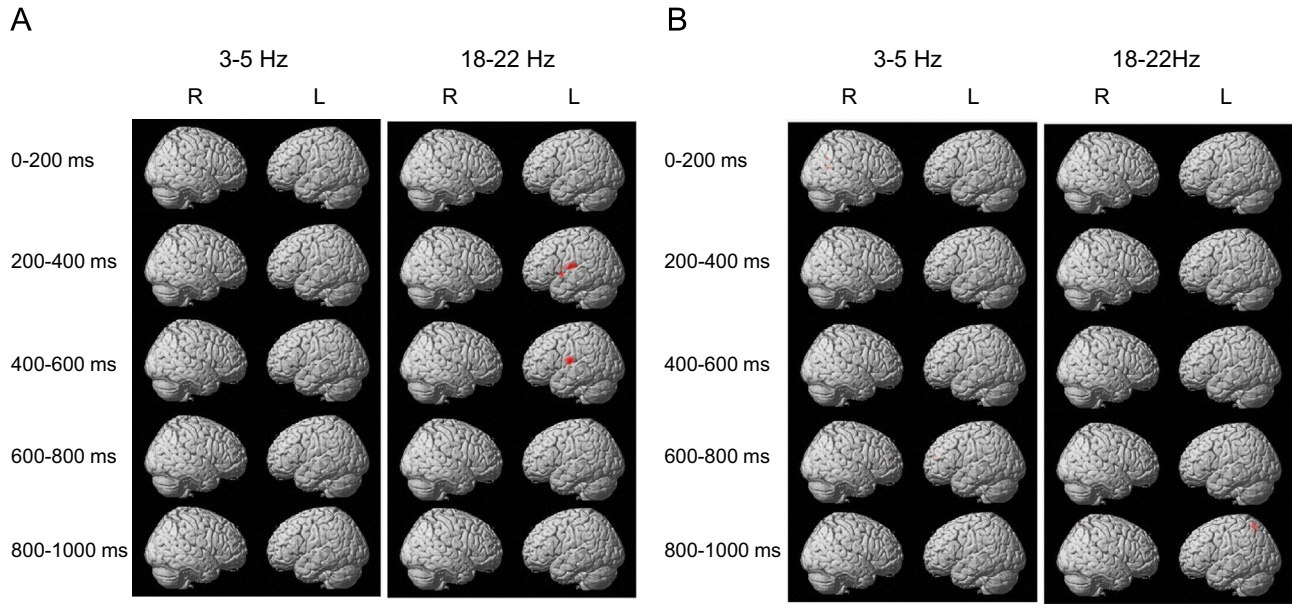

Fig. 4 – Statistical parametric maps of decreased (A) and increased (B) 3–5 Hz and 18–22 Hz band powers in the forward condition relative to the reverse condition (paired *t*-test). Statistical parametric maps are superimposed on surface-rendered high-resolution MRI. Brain regions showing decreased (A) or increased (B) band powers are colored in red. The right (R) and left (L) sides are indicated. Random-effect analyses of 12 participants, $P<0.05$, corrected for the entire search volumes (family-wise error rate).

post-trigger period, and in the left middle temporal gyrus (BA 22) during the total period. Increased 3–5 Hz band powers in the left inferior frontal gyrus (BAs 45, 46, and 47) were commonly observed during the pre- and post-trigger periods ($P<0.05$, corrected for the entire search volumes, family-wise error rate). Decreased 18–22 Hz band powers were not commonly observed in any brain regions. There were no relationships between the story-comprehension levels and the intensities of the neural activity related to the phonemic restoration for speech comprehension.

Table 1 – Time–frequency band power change after onset of white noise relative to baseline in the forward condition compared with the reverse condition.

Location	Side	BA	MNI coordinates (mm)			Z value
			x	y	z	
Decrease (3–5 Hz)						
Decrease (18–22 Hz)						
200–400 ms						
Transverse temporal gyrus	L	42	−63	−17	15	3.66
Superior temporal gyrus	L	22	−58	3	−5	3.54
400–600 ms						
Transverse temporal gyrus	L	42	−63	−12	15	4.32
Increase (3–5 Hz)						
Increase (18–22 Hz)						
800–1000 ms						
Precuneus	L	7	−18	−62	60	4.25

BA, Brodmann's area; MNI, Montréal Neurological Institute; L, Left.
x, y, z: Stereotaxic coordinates.
Random-effect analyses of 12 participants, corrected for the volumes ($P<0.05$, family-wise error rate).

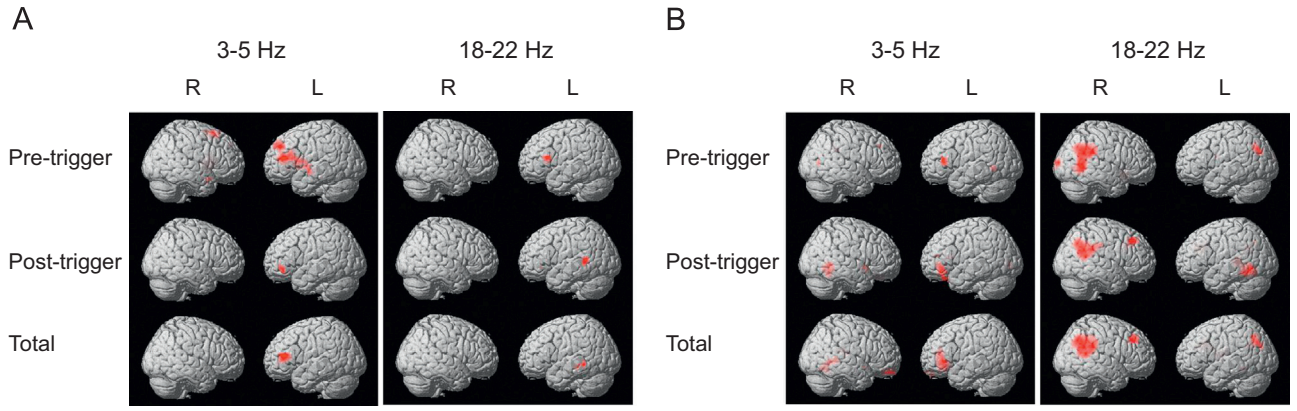

Fig. 5 – Statistical parametric maps of decreased (A) and increased (B) 3–5 Hz and 18–22 Hz band powers in the forward condition relative to the reverse condition during the pre-trigger (−500 to 0 ms), post-trigger (0 to 1000 ms), and total (−500 to 1000 ms) periods (one-sample *t*-test). Statistical parametric maps are superimposed on surface-rendered high-resolution MRI. Brain regions showing decreased (A) or increased (B) band powers are colored in red. The right (R) and left (L) sides are indicated. Random-effect analyses of 12 participants, $P<0.05$, corrected for the entire search volumes.

3. Discussion

We found decreased 18–22 Hz band powers caused by white-noise stimuli in the forward condition compared with the reverse condition in the left transverse and superior temporal gyri and continuously increased 3–5 Hz band power in the left inferior frontal gyrus. These results suggest that the left transverse and superior temporal gyri and the left inferior frontal gyrus are brain regions related to phonemic restoration for speech comprehension.

We identified neural activations in response to the white-noise stimuli during listening to and understanding spoken Japanese stories in the left transverse and superior temporal gyri. Consistent with our results, fMRI studies have demonstrated that the auditory cortex is related to the phonemic restoration. A macaque study showed that the continuity illusion for the missing segment of occluded tonal foregrounds reflects activity of neurons in the auditory cortex (Petkov et al., 2007b), while a human study showed that the perceived continuity of illusionary tones in noise reflects activity in the auditory cortex (Riecke et al., 2007). The transverse and superior temporal gyri respond as a function of stimulus complexity and speech intelligibility (Narain et al., 2003; Liebenthal et al., 2005; Scott et al., 2006), and these brain regions are considered to show the first clear responses to linguistic information and the anatomical implementation of phonemic maps in speech (Rauschecker and Scott, 2009). The left transverse and superior temporal gyri may thus contribute to phonemic restoration for speech comprehension through the function of first processing of speech information. Left-lateralization is a feature related to speech processing (Narain et al., 2003; Scott et al., 2006), and hemispheric specialization was also apparent in our results.

Neural activations during listening to and understanding spoken Japanese stories were seen in the left inferior frontal gyrus (BAs 45, 46, and 47), which includes Broca's area,

Table 2 – Time–frequency band power change in the forward condition compared with the reverse condition during pre-trigger (−500 to 0 ms), post-trigger (0 to 1000 ms), and total (−500 to 1000 ms) periods.

Location	Side	BA	MNI coordinates (mm)			Z value
			x	y	z	
Decrease (3–5 Hz)						
Pre-trigger						
Precentral gyrus	L	44	−53	8	10	4.43
Middle frontal gyrus	L	10	−38	38	15	4.41
Middle frontal gyrus	R	6	32	13	60	4.22
Post-trigger						
Middle frontal gyrus	L	47	−53	43	−5	3.75
Total						
Inferior frontal gyrus	L	46	−48	38	10	4.08
Decrease (18–22 Hz)						
Pre-trigger						
Insula	L	13	−28	23	15	6.13
Post-trigger						
Middle temporal gyrus	L	21	−48	−47	5	4.13
Total						
Middle temporal gyrus	L	22	−53	−42	−5	3.87
Increase (3–5 Hz)						
Pre-trigger						
Inferior frontal gyrus	L	45	−48	28	10	4.24
Middle temporal gyrus	R	39	57	−72	10	3.99
Post-trigger						
Inferior frontal gyrus	L	47	−53	38	−10	4.50
Inferior temporal gyrus	R	37	62	−52	−5	4.17
Total						
Inferior frontal gyrus	L	47	−53	33	−5	5.14
Superior frontal gyrus	R	11	17	53	−20	4.21
Middle occipital gyrus	R	37	62	−62	−10	4.02
Increase (18–22 Hz)						
Pre-trigger						
Angular gyrus	L	39	−48	−72	35	4.20
Supramarginal gyrus	R	40	62	−47	30	4.14
Middle occipital gyrus	R	19	22	−102	10	4.06
Post-trigger						
Supramarginal gyrus	R	40	57	−52	20	4.18
Superior temporal gyrus	L	41	−43	−37	5	4.16
Middle frontal gyrus	R	8	32	38	45	4.09
Total						
Inferior parietal lobule	R	40	57	−62	40	4.19
Inferior parietal lobule	L	39	−48	−67	40	3.98
Middle frontal gyrus	R	8	32	38	45	3.90

BA, Brodmann's area; MNI, Montréal Neurological Institute; R, Right; L, Left.
x, y, z: Stereotaxic coordinates.
Random-effect analyses of 12 participants, corrected for the entire search volumes ($P<0.05$, family-wise error rate).

throughout the pre- and post-trigger periods. An fMRI study demonstrated the high-level cortical mechanisms of phonemic restoration: this process relies on two dissociable neural mechanisms, i.e., the subjective experience of illusory continuity; and the unconscious sensory repair. Broca's area was related to unconscious sensory repair (Shahin et al., 2009). Sensory repair causes reconstruction of low-level sensory representations, where "bottom-up" information is degraded or missing (Petkov et al., 2007a). This includes restoring the information, and should recruit the left inferior frontal gyrus for controlled acoustic sequencing and pattern recognition (Zatorre et al., 1992; Burton et al., 2000; Zaehle et al., 2008). The left inferior frontal gyrus may thus contribute to phonemic restoration for speech comprehension through unconscious sensory repair. Interestingly, although neural activation during listening to and understanding spoken Japanese stories was seen in the left inferior frontal gyrus, peak location shift from BA 45 to BA 47 was observed from the pre-trigger period to post-trigger period. This demonstrates that the activation in the left inferior frontal gyrus was not induced by just listing to the speech. In addition, since BA 45 was related to phonological processing and BA 47 was related to semantic processing (Zhang et al., 2012), the important role of the semantic processing on the phonemic restoration is suggested.

No relationships between the story-comprehension levels and the intensities of the neural activity related to the phonemic restoration for speech comprehension were identified in our present study. One reason why we could not identify the relationships between them may be that the story-comprehension levels did not vary among the participants In fact, they answered the questions about the contents of the Story A and Story B almost perfectly (i.e., they marked 6–8 out of 8 in the questions about the contents of the each story).

While the present results suggest mechanisms for phonemic restoration in speech comprehension, only a limited number of participants were tested. To generalize the results, studies involving a larger number of participants are needed. In addition, assessing the neural activities of brain regions located deeply or frontally was difficult using MEG. Some brain regions involved in phonemic restoration might thus have been missed because of the limitations of MEG. Future studies using other neuroimaging techniques, such as fMRI and PET, would address this limitation.

We found brain activations related to phonemic restoration for speech comprehension. The left transverse and superior temporal gyri activated in response to white-noise stimuli while listening to and understanding the spoken stories, and these brain regions seem to contribute to phonemic restoration for speech comprehension through first processing of speech information. The left inferior frontal gyrus, including Broca's area, was continuously activated throughout listening to and understanding the spoken stories, and this brain region may contribute to phonemic restoration for speech comprehension through unconscious sensory repair. These findings may help clarify the neural mechanisms of phonemic restoration and develop innovative treatment methods such as new linguistic training strategies for individuals who suffer from impaired speech comprehension, particularly in noisy environments.

4. Experimental procedures

4.1. *Participants*

Twelve healthy male volunteers (mean (± standard deviation (SD)) age, 26.36±5.54 years) were enrolled in this study. Current smokers, individuals with a history of medical illness such as neurological disease, psychiatric disease, or developmental disorders including reading disabilities, or individuals taking chronic medications or supplements that affect the central nervous system were excluded from the study. All participants had normal hearing and were right-handed according to the Edinburgh handedness inventory (Oldfield, 1971). Normal hearing was ensured by pure tone audiometry and the speech discrimination test. Conventional pure-tone audiometry and speech audiometry were performed using a diagnostic audiometer (AA-78; RION, Tokyo, Japan) in a sound-proof room to assess hearing acuity. In pure-tone audiometry, pure-tone hearing ability was judged normal when all of air-conduction pure-tone thresholds recorded at 7 audiometric frequencies, octave intervals from 125 to 8000 Hz, did not exceed 20 dB hearing level (HL). In speech audiometry, speech recognition scores were assessed using the list of Japanese monosyllables (67-S word table which was standardized by the Japan Audiological Society) presented at 50 dB HL and speech recognition ability was judged normal when speech recognition scores reached equal to or more than 90%. All participants were native Japanese speakers with higher than college level education. The study protocol was approved by the ethics committee of Osaka City University and was conducted in accordance with the principles of the Declaration of Helsinki, with written informed consent obtained from all participants prior to enrollment in the study.

4.2. *Experimental design*

This study comprised three experimental sessions (Story A session, Story B session, and Story C session) (Fig. 6A). After enrollment, participants were randomly assigned to three groups in a single-blinded, three-crossover fashion to consecutively undergo these three experimental sessions. They were requested to carefully listen to and understand three spoken Japanese stories (Story A, Story B, and Story C) with their eyes closed. The stories were constructed of recorded narratives in which 2–4 syllables of the latter portion of spoken keywords, which seemed to contribute to the understanding of the stories, were replaced by 300-ms white-noise stimuli with an inter-stimulus interval of 1.6–20.3 s (Fig. 6B). Two of the three stories (Story A and Story B) were played forward and one story (Story C) was played in reverse (Story C was the reverse version of Story A). All spoken words consisted of the same digitally recorded female voice. Sound pressure, frequency range, and duration of the spoken words and white noise were adjusted using Adobe Premier Elements (Adobe Systems, Tokyo, Japan) and presented via an MEG-compatible sound system (Model ER-2; Etymotic Research, Elk Grove Village, IL) using Windows Media Player 9 (Microsoft Japan, Tokyo, Japan) implemented on a personal computer (Precision PWS390; Dell Computer, TX). The Story A session involved 50 white-noise stimuli with a total duration of 311 s and the Story B session involved 68 white-noise stimuli with a total duration of 412 s, and the Story A session and the Story B session constituted a forward condition. The Story C session consisted of 101 white-noise stimuli with a total duration of 311 s, and the Story C session constituted a reverse condition. We recorded MEG during these three experimental sessions, and white noise was used as a stimulus. The reverse condition was performed as a control, and we compared MEG responses to white-noise stimuli during the forward condition with those during the reverse condition using time–frequency analyses, in order to investigate neural activations related to phonemic restoration. Immediately after the end of the Story A and Story B sessions, the participants were asked 8 questions about the contents of each story to assess the objective story-comprehension level. Each question comprised 4 choices with one correct answer. In addition, immediately after the end of the questions, participants were also asked to subjectively rate their story-comprehension level on a 5-point scale, ranging from 1 ("I could not understand the story at all") to 5 ("I could totally understand the story"). This study was conducted in a quiet,

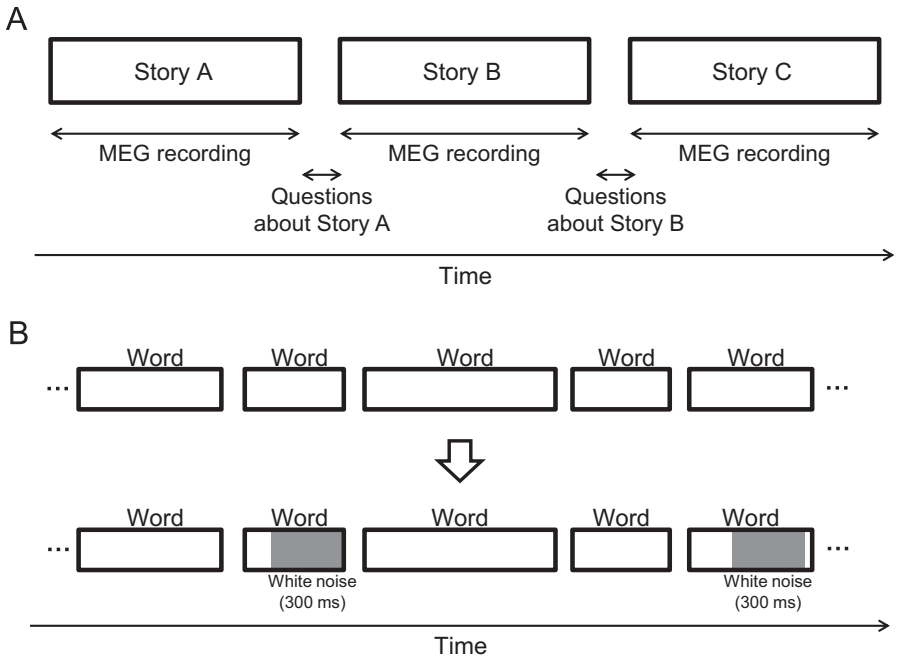

Fig. 6 – Experimental design. (A) Participants performed the experiment in a three-crossover fashion to include three experimental sessions (Story A session, Story B session, and Story C session). They were requested to carefully listen to and understand three spoken Japanese stories (Story A, Story B, and Story C) with their eyes closed. Two of the three stories (Story A and Story B) were played forward and one story (Story C) was played in reverse (Story C was the reverse version of Story A). Magnetoencephalography (MEG) was recorded during these three experimental sessions. Immediately after the end of the Story A and B sessions, subjects were asked 10 and 8 questions about the contents of Story A and Story B, respectively, to assess the objective story-comprehension level. (B) The three stories were constructed of recorded narratives in which 2–4 syllables of the latter portion of spoken keywords, which seemed to contribute to an understanding of the stories, were replaced by 300-ms white-noise stimuli with an inter-stimulus interval of 1.6–20.3 s.

temperature- and humidity-controlled magnetically shielded room at Osaka City University Hospital. For the day before each visit, all participants refrained from intense mental and physical activities and caffeinated beverages, consumed a normal diet and beverages, and maintained normal sleeping hours.

4.3. *MEG recordings*

MEG recordings were performed using a 160-channel whole-head-type MEG system (MEG vision; Yokogawa Electric Corporation, Tokyo, Japan) with a magnetic field resolution of 4 fT/Hz1/2 in the white-noise region. Sensor and reference coils were gradiometers 15.5 mm in diameter and 50 mm in baseline, and each pair of sensor coils was separated by a distance of 23 mm. The sampling rate was 1000 Hz with a 0.3-Hz high-pass filter and 500-Hz low-pass filter.

4.4. *MEG data analyses*

MEG signal data were analyzed offline after analog-to-digital conversion. Magnetic noise originating from outside the shield room was eliminated by subtracting the data obtained from reference coils using MEG 160 software (Yokogawa Electric Corporation) followed by rejection of artifacts by careful visual inspection. MEG data were split into segments of 1500 ms length (from −500 to 1000 ms relative to the onset of each white noise) and the segments were averaged. After averaging, data were band-pass filtered by a fast Fourier transform using Frequency Trend software (Yokogawa Electric Corporation) to obtain time–frequency band signals using Brain Rhythmic Analysis for MEG software (BRAM; Yokogawa Electric Corporation) (Dalal et al., 2008).

Localization and intensity of the time–frequency power of cortical activity were estimated using BRAM software, which used narrow-band adaptive spatial filtering methods as an algorithm (Dalal et al., 2008). These data were then analyzed using Statistical Parametric Mapping (SPM8; Wellcome Department of Cognitive Neurology, London, UK), implemented in Matlab (Mathworks, Sherbon, MA). The MEG anatomical/spatial parameters used to warp the volumetric data were transformed into the Montreal Neurological Institute (MNI) template of T1-weighted images (Evans et al., 1994) and applied to the MEG data. Anatomically normalized MEG data were filtered with a Gaussian kernel of 20 mm (full-width at half-maximum) in the x, y, and z axes (voxel dimension, $5.0 \times 5.0 \times 5.0\ mm^3$). Oscillatory power for each frequency band and time window in the forward condition relative to the reverse condition was measured on a region-of-interest basis to obtain the neural activation pattern of the phonemic restoration for speech comprehension. The resulting set of voxel values for each comparison constituted a SPM of *t*-statistics (SPM{*t*}). SPM{*t*} was transformed to the unit of normal distribution (SPM{*Z*}). The threshold for the SPM{*Z*} of individual

analyses was set at $P<0.05$ (corrected for multiple comparisons). The weighted sum of parameters estimated in the individual analyses consisted of "contrast" images, which were used for group analyses (Friston et al., 1999). So that inferences could be made at a population level, individual data were summarized and incorporated into a random-effect model (Friston et al., 1999). SPM{t} and SPM{Z} for contrast images were created as described above. Significant signal changes for each contrast were assessed by means of *t*-statistics on a voxel-by-voxel basis (Friston et al., 1999). The threshold for the SPM{Z} of group analyses was set at $P<0.05$ (corrected for multiple comparisons). Anatomical localizations of significant voxels within clusters were achieved using Talairach Demon software (Lancaster et al., 2000).

4.5. *MRI overlay*

Anatomical MRI was performed using a Philips Achieva 3.0TX (Royal Philips Electronics, Eindhoven, the Netherlands) to permit registration of magnetic source locations with their respective anatomical locations. Before MRI, five adhesive markers (Medtronic Surgical Navigation Technologies, Broomfield, CO) were attached to the skin of the participant's head (first and second markers located at 10 mm in front of the left tragus and right tragus, third at 35 mm above the nasion, and fourth and fifth at 40 mm to the right and left of the third marker). MEG data were superimposed on MR images using information obtained from these markers and the MEG localization coils.

4.6. *Statistical analyses*

Data are presented as mean±SD unless otherwise stated. All *P* values were two-tailed, and values less than 0.05 were considered statistically significant. Statistical analyses were performed using IBM SPSS 20.0 software (IBM, Armonk, NY).

Acknowledgments

We wish to thank Manryoukai Imaging Clinic for performing MRI and Forte Science Communications for editorial help with the manuscript.

REFERENCES

Başkent, D., 2010. Phonemic restoration in sensorineural hearing loss does not depend on baseline speech perception scores. J. Acoust. Soc. Am. 128 (4), 169–174.

Başkent, D., Eiler, C.L., Edwards, B., 2010. Phonemic restoration by hearing-impaired listeners with mild to moderate sensorineural hearing loss. Hear. Res. 260 (1–2), 54–62.

Brookes, M.J., Wood, J.R., Stevenson, C.M., Zumer, J.M., White, T.P., Liddle, P.F., Morris, P.G., 2011. Changes in brain network activity during working memory tasks: a magnetoencephalography study. Neuroimage 55 (4), 1804–1815.

Burton, M.W., Small, S.L., Blumstein, S.E., 2000. The role of segmentation in phonological processing: an fMRI investigation. J. Cogn. Neurosci. 12 (4), 679–690.

Dalal, S.S., Guggisberg, A.G., Edwards, E., Sekihara, K., Findlay, A.M., Canolty, R.T., Berger, M.S., Knight, R.T., Barbaro, N.M., Kirsch, H.E., Nagarajan, S., 2008. Five-dimensional neuroimaging: localization of the time–frequency dynamics of cortical activity. NeuroImage 40 (4), 1686–1700.

Davis, M.H., Johnsrude, I.S., 2007. Hearing speech sounds: top-down influences on the interface between audition and speech perception. Hear. Res. 229 (1–2), 132–147.

Dubno, J.R., Dirks, D.D., Morgan, D.E., 1984. Effects of age and mild hearing loss on speech recognition in noise. J. Acoust. Soc. Am. 76 (1), 87–96.

Duquesnoy, A.J., 1983. Effect of a single interfering noise or speech source upon the binaural sentence intelligibility of aged persons. J. Acoust. Soc. Am. 74 (3), 739–743.

Evans, A.C., Kamber, M., Collins, D.L., MacDonald, D., 1994. An MRI-based probablistic atlas of neuroanatomy. In: Shorvon, S.D. (Ed.), Magnetic Resonance Scanning and Epilepsy. Plenum Press, New York, pp. 263–274.

Friston, K.J., Holmes, A.P., Worsley, K.J., 1999. How many subjects constitute a study?. NeuroImage 10 (1), 1–5.

Jerger, J., Jerger, S., Oliver, T., Pirozzolo, F., 1989. Speech understanding in the elderly. Ear Hear. 10 (2), 79–89.

Lancaster, J.L., Woldorff, M.G., Parsons, L.M., Liotti, M., Freitas, C.S., Rainey, L., Kochunov, P.V., Nickerson, D., Mikiten, S.A., Fox, P.T., 2000. Automated Talairach atlas labels for functional brain mapping. Hum. Brain Mapp. 10 (3), 120–131.

Liebenthal, E., Binder, J.R., Spitzer, S.M., Possing, E.T., Medler, D.A., 2005. Neural substrates of phonemic perception. Cereb. Cortex 15 (10), 1621–1631.

Narain, C., Scott, S.K., Wise, R.J., Rosen, S., Leff, A., Iversen, S.D., Matthews, P.M., 2003. Defining a left-lateralized response specific to intelligible speech using fMRI. Cereb. Cortex 13 (12), 1362–1368.

Oldfield, R.C., 1971. The assessment and analysis of handedness: the Edinburgh inventory. Neuropsychologia 9 (1), 97–113.

Petkov, C.I., O'Connor, K.N., Sutter, M.L., 2007a. Encoding of illusory continuity in primary auditory cortex. Neuron 54 (1), 153–165.

Petkov, C.I., O'Connor, K.N., Sutter, M.L., 2007b. Encoding of illusory continuity in primary auditory cortex. Neuron 54 (1), 153–165.

Plomp, R., Mimpen, A.M., 1979. Speech-reception threshold for sentences as a function of age and noise level. J. Acoust. Soc. Am. 66 (5), 1333–1342.

Rauschecker, J.P., Scott, S.K., 2009. Maps and streams in the auditory cortex: nonhuman primates illuminate human speech processing. Nat. Neurosci. 12 (6), 718–724.

Riecke, L., van Opstal, A.J., Goebel, R., Formisano, E., 2007. Hearing illusory sounds in noise: sensory-perceptual transformations in primary auditory cortex. J. Neurosci. 27 (46), 12684–12689.

Schneider, B.A., Daneman, M., Murphy, D.R., See, S.K., 2000. Listening to discourse in distracting settings: the effects of aging. Psychol. Aging 15 (1), 110–125.

Scott, S.K., Rosen, S., Lang, H., Wise, R.J., 2006. Neural correlates of intelligibility in speech investigated with noise vocoded speech—a positron emission tomography study. J. Acoust. Soc. Am. 120 (2), 1075–1083.

Shahin, A.J., Bishop, C.W., Miller, L.M., 2009. Neural mechanisms for illusory filling-in of degraded speech. Neuroimage 44 (3), 1133–1143.

Sivonen, P., Maess, B., Lattner, S., Friederici, AD., 2006. Phonemic restoration in a sentence context: evidence from early and late ERP effects. Brain Res. 1121 (1), 177–189.

Stam, C.J., 2010. Use of magnetoencephalography (MEG) to study functional brain networks in neurodegenerative disorders. J. Neurol. Sci 289 (1–2), 128–134.

Varela, F., Lachaux, J.P., Rodriguez, E., Martinerie, J., 2001. The brainweb: phase synchronization and large-scale integration. Nat. Rev. Neurosci. 2 (4), 229–239.

Verschuure, J., Brocaar, M.P., 1983. Intelligibility of interrupted meaningful and nonsense speech with and without intervening noise. Percept. Psychophys. 33 (3), 232–240.
Warren, R.M., 1970. Perceptual restoration of missing speech sounds. Science 167 (3917), 392–393.
Warren, R.M., Obusek, C.J., Ackroff, J.M., 1972. Auditory induction: perceptual synthesis of absent sounds. Science 176 (4039), 1149–1151.
Warren, R.M., Bashford Jr., J.A., 1981. Perception of acoustic iterance: pitch and infrapitch. Percept. Psychophys. 29 (4), 395–402.
Warren, R.M., Hainsworth, K.R., Brubaker, B.S., Bashford Jr., J.A., Healy, E.W., 1997. Spectral restoration of speech: intelligibility is increased by inserting noise in spectral gaps. Percept. Psychophys. 59 (2), 275–283.
Zaehle, T., Geiser, E., Alter, K., Jancke, L., Meyer, M., 2008. Segmental processing in the human auditory dorsal stream. Brain Res. 1220, 179–190.
Zatorre, R.J., Evans, A.C., Meyer, E., Gjedde, A., 1992. Lateralization of phonetic and pitch discrimination in speech processing. Science 256 (5058), 846–849.
Zhang, J.X., Xiao, Z., Weng, X., 2012. Neural evidence for direct meaning access from orthography in Chinese word reading. Int. J. Psychophysiol. 84 (3), 240–245.